9

Variational Monte Carlo

One of the reasons for the popularity of the variational Monte Carlo method is its versatility. It can be used to calculate the ground state properties of Fermion, Boson, and quantum spin systems without suffering from a sign problem. Even computing a few excited states is sometimes possible. While we can use this method as an independent quantum Monte Carlo method, we frequently resort to variational Monte Carlo calculations to generate an optimized trial state that becomes the starting point for other ground state methods. We discuss these other methods in Chapters 10 and 11. Here, we detail the variational Monte Carlo method, emphasizing its foundations and surveying the types of trial states often used. We also discuss the techniques used for the optimization of the trial state.

9.1 Variational Monte Carlo

9.1.1 The variational principle

In its simplest form, the variational Monte Carlo method uses Monte Carlo sampling to estimate the integrals implied in the Rayleigh-Ritz variational bound for the ground state energy,

$$E_0 \leq E_T = \frac{\langle \psi_T | H | \psi_T \rangle}{\langle \psi_T | \psi_T \rangle}, \tag{9.1}$$

and uses a deterministic or empirical method to adjust the trial-state's parameters to bring E_T as close to E_0 as possible. We first establish the variational principle.

Let us suppose that we are given a trial state $|\psi_T\rangle$ that is a good estimate of some eigenstate of a Hamiltonian H, an eigenstate that may or may not be the ground state. Because this trial state is in general not an eigenstate, we cannot use the standard eigenvalue-eigenstate relation $H|\psi_T\rangle = E_T|\psi_T\rangle$ to associate an energy E_T with $|\psi_T\rangle$. We may however define the residual state

https://doi.org/10.1017/CBO9780511902581.010 Published online by Cambridge University Press

$$|\phi\rangle = (H - E_T)\,|\psi_T\rangle\,,$$

whose norm provides a measure of how far $|\psi_T\rangle$ is from a true eigenstate with energy E_T. Clearly, this norm is zero only when E_T and $|\psi_T\rangle$ are some eigenpair of H. If $|\psi_T\rangle$ is not an eigenstate, we instead seek a value of E_T that minimizes the norm

$$\langle\phi|\phi\rangle = \langle (H - E_T)\psi_T | (H - E_T)\psi_T\rangle\,. \tag{9.2}$$

From (9.2) we have

$$\langle\phi|\phi\rangle = \langle H\psi_T|H\psi_T\rangle - E_T\,\langle H\psi_T|\psi_T\rangle - E_T\,\langle\psi_T|H\psi_T\rangle + E_T^2,$$

which after defining $\lambda = \langle\psi_T|H\psi_T\rangle / \langle\psi_T|\psi_T\rangle$ becomes

$$\langle\phi|\phi\rangle = \langle H\psi_T|H\psi_T\rangle + \langle\psi_T|\psi_T\rangle\left[(E_T - \lambda)^2 - \lambda^2\right]. \tag{9.3}$$

Because both $\langle H\psi_T|H\psi_T\rangle$ and $\langle\psi_T|\psi_T\rangle$ are positive, we minimize (9.3) by choosing E_T so that the expression in the brackets is as negative as possible. The choice

$$E_T = \lambda = \frac{\langle\psi_T|H\psi_T\rangle}{\langle\psi_T|\psi_T\rangle}$$

does this, and since H is Hermitian, we can finally write

$$E_T = \frac{\langle\psi_T|H|\psi_T\rangle}{\langle\psi_T|\psi_T\rangle}. \tag{9.4}$$

The ratio on the right-hand side is called *Rayleigh's quotient*. Its numeric value is E_T.

A standard result from linear algebra is that the minimum and maximum eigenvalues of H bound Rayleigh's quotient. To show this, we first let $E_0, E_1, \ldots, E_N$ be the eigenvalues of H in ascending order. Expressing $|\psi_T\rangle$ as a linear combination of the corresponding orthonormal eigenvectors $|\psi_i\rangle$, we have

$$E_T = \frac{\sum_{ij} a_i^* a_j \langle\psi_i\,|H|\,\psi_j\rangle}{\sum_{ij} a_i^* a_j\,\langle\psi_i\mid\psi_i\rangle} = \frac{\sum_i |a_i|^2 E_i}{\sum_i |a_i|^2}.$$

Now,

$$E_0 = \frac{\sum_i |a_i|^2 E_0}{\sum_i |a_i|^2}, \quad E_N = \frac{\sum_i |a_i|^2 E_N}{\sum_i |a_i|^2},$$

so that

$$E_0 - E_T = \frac{\sum_i |a_i|^2\,(E_0 - E_i)}{\sum_i |a_i|^2} \leq 0,$$

$$E_N - E_T = \frac{\sum_i |a_i|^2\,(E_N - E_i)}{\sum_i |a_i|^2} \geq 0,$$

https://doi.org/10.1017/CBO9780511902581.010 Published online by Cambridge University Press

or

$$E_0 \leq E_T \leq E_N.$$

This is a pretty powerful result, as the Rayleigh quotient for any admissible trial function must satisfy these bounds.

There are several facts that follow from the Rayleigh quotient that deserve mention. The first is that if the trial state is accurate to $\mathcal{O}(\varepsilon)$, where ε is small, then the variational energy E_T is accurate to $\mathcal{O}(\varepsilon^2)$; that is, it is accurate to a higher order. Thus, making $|\psi_T\rangle$ as close to $|\psi_0\rangle$ as possible makes E_T even closer to E_0. However, on the flip side of the coin, a value of E_T close to E_0 does not necessarily mean that $|\psi_T\rangle$ represents the physics of $|\psi_0\rangle$ as accurately as we might hope.

The second fact, or more accurately a set of related facts, has to do with the convergence to an optimal energy as a function of the parameters of the trial wave function. If the set of parameters for the trial wave function were $p = (p_1, p_2, \ldots, p_{N_{\text{opt}}})$, then we would hope that increasing the number of parameters yields a sequence $E_0 \leq \cdots \leq E_T(p_1, p_2, p_3) \leq E_T(p_1, p_2) \leq E_T(p_1)$. For example, if the ground state has a single peak in a limited region of phase space, then we would expect a trial state parameterized by the location and width of a Gaussian would yield a lower energy than a trial state parameterized by just the location or the width of a Gaussian. With just one parameter, we would need a good guess of the other to do as well as using two parameters.

One case where we can prove the systematic convergence of the trial state with increasing number of parameters is the case where we express the trial state as a linear combination of n basis states. Any basis spanning the Hilbert space of the given Hamiltonian will do. If the dimension of this space is N, but we construct a trial state $|\psi_T\rangle = \sum_{i=1}^{n} p_i |\phi_i\rangle$, where $\{|\phi_i\rangle\}_{i=1}^{N}$ is some basis in the Hilbert space, which is not necessarily orthogonal, then for $n < N$ we can show that the set of parameters $\{p_i\}_{i=1}^{n}$ that minimizes the Rayleigh quotient satisfies the generalized eigenvalue problem

$$Hp = \lambda Sp,$$

where we define the Hamiltonian matrix H and overlap matrix S by

$$H_{ij} = \langle \phi_i | H | \phi_j \rangle \text{ and } S_{ij} = \langle \phi_i | \phi_j \rangle.$$

The overlap matrix is positive-definite.

If the basis is orthonormal, then the overlap matrix is the identity matrix, and we recover the standard eigenvalue equation. We could have obtained this same equation by minimizing the quadratic form $Q = \sum_{ij} H_{ij} p_i p_j$ subject to the constraint $\sum_i p_i^2 = 1$. Let $\lambda_1 \leq \lambda_2 \leq \cdots \leq \lambda_n$ be the eigenvalues of Q. Next, suppose we reduce Q by j linear, homogeneous constraints to a quadratic form $\bar{Q}$ whose

eigenvalues are $\bar{\lambda}_1 \leq \bar{\lambda}_2 \leq \cdots \leq \bar{\lambda}_{n-j}$. Then we have (Courant and Hilbert, 1965)

$$\lambda_1 \leq \bar{\lambda}_1 \leq \lambda_2 \leq \bar{\lambda}_2 \cdots \leq \bar{\lambda}_{n-j} \leq \lambda_{n+1-j}. \tag{9.5}$$

In particular, if we take $j = 1$ and $p_n = 0$, then the quadratic form Q goes to that of its first principal minor, and thus we have the result that the i-th eigenvalue of the first principal minor is at least equal to the i-th eigenvalue of the original quadratic form and at most equal to the original $(i + 1)$-th eigenvalue. We obtain a similar interlacing of eigenvalues if we repeat this process and reduce the $(n - 1)$-minor to the $(n - 2)$-minor. The importance of these interlacing results is that within the Rayleigh variational framework, we need to use a basis at least of order n to be able to bound the n-th exact eigenvalue. If we increase the basis from n to $n + 1$, we have that

$$\lambda_i \leq \lambda_i(n + 1) \leq \lambda_i(n) \leq \lambda_{i+1}$$

for a general adjacent pair of exact eigenvalues. If we keep increasing the number of basis functions, as $n \to N$, we converge to the exact result.

In Section 9.2, we discuss various common options for the choice of many-body trial states. In some cases the trial state is a single state embodying all the parameters. In others, it is a linear combination of basis states. In still others, it could be a mix of the two other cases. In Section 9.3, we present a numerical technique to execute the minimization for the mixed case. Next we discuss the basics of using the Monte Carlo method in the variational method.

9.1.2 Monte Carlo sampling

We now discuss how to evaluate (9.4) by a Monte Carlo method. With a complete orthonormal basis $\{|C\rangle\}$ satisfying $\sum_C |C\rangle\langle C| = I$ and $\langle C|C'\rangle = \delta_{CC'}$, which we call the *configuration basis*, (9.4) becomes

$$E_T = \frac{\sum_C \langle \psi_T|C\rangle \, \langle C|H|\psi_T\rangle}{\sum_C |\langle C|\psi_T\rangle|^2}.$$

We rewrite this as

$$E_T = \sum_C E\,(C) p\,(C)$$

with

$$E(C) = \frac{\langle C|H|\psi_T\rangle}{\langle C|\psi_T\rangle} \quad \text{and} \quad p(C) = \frac{|\langle C|\psi_T\rangle|^2}{\sum_C |\langle C|\psi_T\rangle|^2}.$$

https://doi.org/10.1017/CBO9780511902581.010 Published online by Cambridge University Press

$E(C)$ is called the *configuration energy*. Sampling configurations from $p(C)$ allows us to invoke the standard Monte Carlo estimate for the variational energy:

$$E_T \approx \bar{E}_T \equiv \frac{1}{M}\sum_{i=1}^{M} E(C_i). \tag{9.6}$$

We can use the Metropolis-Hastings (2.28) or a similar algorithm to sample the configurations C_i from $p(C)$. These algorithms require a user-defined proposal probability $T(C'|C)$ for changing the state $|C\rangle$ to $|C'\rangle$. We recall that the Metropolis-Hastings algorithm then *fixes* the acceptance probability $A(C'|C)$ for the proposed change to be

$$A(C' \leftarrow C) = \min\left\{1, \frac{p(C')T(C|C')}{p(C)T(C'|C)}\right\} = \min\left\{1, \frac{|\langle C'|\psi_T\rangle|^2 T(C|C')}{|\langle C|\psi_T\rangle|^2 T(C'|C)}\right\}.$$

With the same samples, we may estimate other observables by

$$\langle \mathcal{O}\rangle \approx \frac{1}{M}\sum_{i=1}^{M} \mathcal{O}(C_i), \tag{9.7a}$$

with

$$\mathcal{O}(C) = \frac{\langle C|\mathcal{O}|\psi_T\rangle}{\langle C|\psi_T\rangle}. \tag{9.7b}$$

In general, these other estimates are not variational bounds.

While the energy variational functional (9.1) is a natural starting point for optimizing a trial state, other choices are possible and at times lead to more convenient and efficient algorithms. The most common alternative uses the definition of the variance of the energy associated with H and $|\psi_T\rangle$ (Umrigar et al., 1988),

$$\sigma_E^2 \equiv \frac{\langle \phi|\phi\rangle}{\langle \psi_T|\psi_T\rangle} = \frac{\langle \psi_T|(H-E_T)^2|\psi_T\rangle}{\langle \psi_T|\psi_T\rangle}. \tag{9.8}$$

This functional is actually the same as the one we used to derive the energy variational functional (9.2). It makes explicit the fact that as $|\psi_T\rangle$ converges to the ground state, the energy variance, associated with the Rayleigh quotient, converges to zero. This fact is called the *zero variance principle*.[1] The zero variance principle also has a Monte Carlo implication: As $|\psi_T\rangle$ converges to the ground state, the configurational energy $E(C)$ converges to the ground state energy E_0 and hence becomes independent of the configurations. If it is independent of the configurations, it has zero variance.

[1] We note that the zero variance property is true for any eigenstate and not just the ground state.

https://doi.org/10.1017/CBO9780511902581.010 Published online by Cambridge University Press

Zero is a lower bound of (9.8), and its having a known lower bound is a feature distinguishing a variational calculation based on the variance functional from one based on the energy functional (9.1). While a lower bound for the energy functional exists, it is unknown.

We can easily show that

$$\sigma_E^2 = \sum_C [E(C) - E_T]^2 p(C),$$

with

$$E_T = \sum_C E(C)p(C) \quad \text{and} \quad p(C) = \frac{|\langle C|\psi_T\rangle|^2}{\sum_C |\langle C|\psi_T\rangle|^2}.$$

This implies that the variance computation requires the same energy estimator and sampling as the calculation based on (9.4), not a surprising result because the Rayleigh quotient is the energy estimator that minimizes the energy variance. Formally, as $|\psi_T\rangle \to |\psi_0\rangle$, the two functionals yield the same E_T and $|\psi_T\rangle$, that is, they both yield E_0 and $|\psi_0\rangle$. In practice, the computational efficiency of the two can vary widely.

Ideally, the variational Monte Carlo method would use a readily available $|\psi_T\rangle$, which is as good an estimate of $|\psi_0\rangle$ as possible. After running the simulation, the job is done. Typically, a good guess has a set of adjustable parameters. If the number of parameters is small, the minimum is most easily found graphically. If the number of parameters is large, a combination of Monte Carlo and deterministic methods is necessary. In this combination, the energy is estimated simultaneously with the optimization of the wave function; that is, we do not first optimize the wave function and then estimate the energy.

In the next section we discuss the different classes of trial states that have proven useful in variational Monte Carlo simulations of lattice models. Then, in Section 9.3, we discuss a procedure to optimize the trial state. As the parameterization of the trial states becomes more complex, this procedure becomes more useful.

9.2 Trial states

The use of trial states gives the variational Monte Carlo method, and any variational calculation for that matter, a "what you get out is what you put in" character. This character manifests itself in two ways. First, if we know the symmetry of the ground state and construct a trial state matching it, then we can bring the variational energy as close to the ground state energy as possible by increasing the parameterization of the trial state. How close we get depends on how much effort we put into crafting the trial state. For quantum lattice problems, we typically know only the symmetries

https://doi.org/10.1017/CBO9780511902581.010 Published online by Cambridge University Press

of the Hamiltonian and are interested in whether one of these symmetries breaks. The variational calculation, however, does not break symmetries.

A vexing problem with a variational calculation is that while different *Ansätze* for the ground state may be orthogonal, their variational energies may be nearly identical. Which one is the correct state? Unfortunately, even if the energies differ significantly, we cannot conclude that the state with lower energy necessarily represents the ground state. Choosing an appropriate ansatz for the ground state requires additional information. In general, we craft the trial state to embrace whatever we exactly know about the ground state and then experiment. This exact information may be just that the ground state is real and square integrable.

Researchers working on electronic structure calculations for atoms, molecules, and solids in the continuum, confident that its ground state is a spin singlet, have finely honed the variational Monte Carlo method by developing powerful procedures to optimize trial states with a large number of parameters. While a variational Monte Carlo simulation on a lattice shares many of the challenges of one in the continuum, an additional complexity arises by the need to compute well more than the ground state energy. Probing novel phases of matter is one need; identifying possible quantum phase transitions is another. Addressing both these needs requires computing correlation functions very accurately. Additionally, besides models for electronic properties, lattice models for quantum spins and Bosons have to be considered. Accordingly, the lattice simulations require more classes of trial states. In the electronic continuum, up to recently, there has been the Slater-Jastrow trial state, but as we will see, this situation is evolving. We start our discussion of trial states by discussing this Slater-Jastrow class as a point for comparison and contrast, and then we discuss several classes of trial states useful for lattice models. Several of these functions have a form similar to the Slater-Jastrow construction, but others evoke quite different concepts.

9.2.1 Slater-Jastrow states

Variational Monte Carlo calculations of the electronic structure of atoms, molecules, and solids use a Slater-Jastrow trial state. In a first quantized representation this state has the form

$$\psi_T(R) = e^{J(R)} D(R),$$

where R represents the spatial coordinates $(r_1, r_2, \ldots, r_N)$ of N electrons, $J(R)$ is the Jastrow function, and $D(R)$ is a Slater determinant. A common Jastrow function has the form

$$J(R) = \sum_{i=1}^{N} \sum_{i<j}^{N} \frac{a_1 r_{ij} + a_2 r_{ij}^2 + \cdots}{1 + b_1 r_{ij} + b_2 r_{ij}^2 + \cdots}, \tag{9.9}$$

https://doi.org/10.1017/CBO9780511902581.010 Published online by Cambridge University Press

where $r_{ij} = |r_i - r_j|$, although more elaborate ones are currently being used. The *Slater determinant* is the product of a spin-up and spin-down determinant,

$$D(R) = \det\left[\psi_n^{\uparrow}(r_{i\uparrow})\right] \det\left[\psi_m^{\downarrow}(r_{j\downarrow})\right],$$

where $\psi_n^{\uparrow}$ and $\psi_m^{\downarrow}$ are single-particle orbitals for up- and down-spin electrons. The $\psi_n^{\sigma}(r_{i\sigma})$ in the arguments of the determinants signify a $N_\sigma \times N_\sigma$ matrix built from these orbitals. More generally,

$$D(R) = \sum_k d_k \det\left[\psi_{k,n}^{\uparrow}(r_{i\uparrow})\right] \det\left[\psi_{k,m}^{\downarrow}(r_{j\downarrow})\right]. \tag{9.10}$$

In a given application, we fix the Slater-Jastrow parameters so the trial state satisfies translational and rotational symmetries. An essential symmetry is the coordinate antisymmetrization the Pauli exclusion principle requires with respect to exchanges of electrons with the same spin. The Slater determinants clearly respect this, but for the complete trial state to do so, the Jastrow factor must be symmetric (Bosonic) with respect to such changes.

The determinants have the form of a single-electron approximation to the many-electron problem. We try to construct them by using the best possible single-particle orbitals for the physical system at hand. In principle, using relatively arbitrary functional forms is possible. In practice, we use the solutions of some mean-field theory. Mean-field theories, such as Hartree-Fock, fail to capture electron correlations adequately. The purpose of the Jastrow factor is to remedy this deficiency. For example, one important use of the Jastrow factor is capturing the correlation energy in the cusp of the wave function caused by the interaction of the electrons with the nuclei.

Typically the parameters of an assumed functional form, such as (9.9), determine the Jastrow function, while the Slater determinants contain the parameters modeling the single-particle orbitals. Both E_T and ψ_T inherit the nonlinear dependence on the parameters of the Jastrow factor and Slater determinant. The only ostensible linear dependence is on the d_k coefficients if we use a multiple state determinant ansatz (9.10).

9.2.2 Gutzwiller projected states

Hubbard model

For electronic lattice problems, the Gutzwiller trial state has a form analogous to the Slater-Jastrow trial state. Gutzwiller proposed this state in conjunction with his proposal for a multi-electron model for ferromagnetism that we now call the *Hubbard model* (Gutzwiller, 1965),

https://doi.org/10.1017/CBO9780511902581.010 Published online by Cambridge University Press

$$H = \sum_{k\sigma} \varepsilon_k n_{k\sigma} + U \sum_i n_{i\uparrow} n_{i\downarrow}. \tag{9.11}$$

The Gutzwiller trial state has the form

$$|\psi_T\rangle = P_G |\psi_0\rangle , \tag{9.12}$$

where the projector P_G is defined as

$$P_G = \exp\left[-\eta \sum_i n_{i\uparrow} n_{i\downarrow}\right] = \prod_i \left[1 - (1-g)\, n_{i\uparrow} n_{i\downarrow}\right]. \tag{9.13}$$

Here, $g = \exp(-\eta)$ and $|\psi_0\rangle$ is some estimate of the ground state. By adjusting g, we can adjust the contribution of the double occupancy in $|\psi_0\rangle$ to the ground state energy estimate. From the definition of P_G, we see that when $g = 1$, it does not project out any double occupancy, but when $g = 0$, it projects out all of it. In principle, we could make the replacement $g \to g_i$. In practice, this is rarely done.

Frequently, we use some Hartree-Fock approximation to guide the selection of the orbitals defining $|\psi_0\rangle$. In Hartree-Fock, we replace the terms in the potential energy, which are quartic in the creation and destruction operators, by ones that are quadratic. For example, we could approximate (9.11) as

$$H \approx \sum_{k\sigma} \varepsilon_k n_{k\sigma} + U \sum_i \left[n_{i\uparrow} \langle n_{i\downarrow}\rangle + n_{i\downarrow} \langle n_{i\uparrow}\rangle\right] - U \sum_i \langle n_{i\uparrow}\rangle \langle n_{i\downarrow}\rangle. \tag{9.14}$$

A Bogoliubov transformation (Blaizot and Ripka, 1986) formally diagonalizes the new quadratic form by defining creation and destruction operators that are linear combinations of the old ones. The new quadratic form, however, contains unknown scalar quantities, such as the $\langle n_{i\sigma}\rangle$ in the above formula. In deterministic uses of such approximations, these scalars constitute the set of parameters we determine self-consistently. In variational Monte Carlo calculations, instead of choosing their values self-consistently, we adjust them to minimize the energy.

We often make various assumptions to reduce the number of parameters. For example, if we assume that the $\langle n_{i\sigma}\rangle$ in (9.14) are independent of i and σ, we obtain the *restricted Hartree-Fock approximation*, which has the single unknown $\langle n\rangle$. In this case, the orbitals are plane waves, and for $|\psi_0\rangle$ we choose the Fermi sea $|FS\rangle$. To construct it, we define creation operators $\alpha^\dagger_{k\sigma}$ for putting an electron of spin σ into a plane-wave state of wave number k. These operators are simply the Fourier transform of the original operators:

$$\alpha^\dagger_{k\sigma} = \frac{1}{\sqrt{V}} \sum_\ell \exp(ik\ell)\; c^\dagger_{\ell\sigma}.$$

https://doi.org/10.1017/CBO9780511902581.010 Published online by Cambridge University Press

The *Fermi sea* is

$$|FS\rangle = \prod_k \alpha_{k\uparrow}^\dagger \prod_k \alpha_{k\downarrow} |0\rangle . \tag{9.15}$$

In restricted Hartee-Fock, the orbitals are independent of $\langle n \rangle$. To adjust $\langle n \rangle$, we simply need to cut off the products in (9.15) so the number of occupied lowest energy states equals the number of electrons. Our variational state then has g as the only adjustable parameter. In this case, the power of variational Monte Carlo is limited to estimating the energy without further approximation, avoiding, for example, the commonly used Gutzwiller approximation (Gutzwiller, 1965; Fazekas, 1999).

Making $\langle n_{i\sigma} \rangle$ independent of i, leaving $\langle n_\sigma \rangle$ unknown, yields the *unrestricted Hartree-Fock approximation*. The unrestricted Hartree-Fock approximation is useful for studying magnetic ground states. Such states have a well-defined wave number K signifying a ferromagnetic, antiferromagnetic, or incommensurate state of long-range magnetic order. The spin-density wave picture is in many respects more useful. For an antiferromagnetic spin-density-wave, for example, we take for $|\psi_0\rangle$ (Yokoyama and Shiba, 1987b)

$$|SDW\rangle = \prod_k d_{k\uparrow}^\dagger d_{k\downarrow}^\dagger |0\rangle, \tag{9.16}$$

where

$$d_{k\uparrow}^\dagger = \alpha_k c_{k\uparrow}^\dagger + \beta_k c_{k+K,\uparrow}^\dagger, \quad d_{k\downarrow}^\dagger = \alpha_k c_{k\downarrow}^\dagger - \beta_k c_{k+K,\downarrow}^\dagger \tag{9.17}$$

with

$$\alpha_k^2 = \frac{1}{2}\left(1 + \frac{\varepsilon_k}{E_k}\right), \quad \beta_k^2 = \frac{1}{2}\left(1 - \frac{\varepsilon_k}{E_k}\right), \tag{9.18}$$

and $E_k = \sqrt{\varepsilon_k^2 + \Delta^2}$ (Δ is a variational parameter). For a two-dimensional square lattice, $K = (\pi, \pi)$.

When we expect superconducting pairing correlations, we take guidance from still another type of Hartree-Fock approximation. Here, we appeal to the BCS theory of superconductivity and take for $|\psi_0\rangle$

$$|BCS\rangle = \prod_k \left(u_k + v_k c_{k\uparrow}^\dagger c_{-k\downarrow}^\dagger\right) |0\rangle , \tag{9.19}$$

where

$$u_k^2 = \frac{1}{2}\left(1 + \frac{\varepsilon_k}{E_k}\right), \quad v_k^2 = \frac{1}{2}\left(1 - \frac{\varepsilon_k}{E_k}\right), \tag{9.20}$$

and $E_k = \sqrt{\varepsilon_k^2 + \Delta_k^2}$. The parameterization of Δ_k is usually made simple with a k-dependence reflecting a particular partial wave. For example, for d-wave symmetry in two dimensions, $\Delta_k = \Delta(\cos k_x - \cos k_y)$.

We emphasize that in both (9.18) and (9.20), Δ is a variational parameter, not an order parameter as would be the case in Hartree-Fock theory. In these latter two trial states, Δ is a parameter that on adjustment hopefully helps to capture the ground state physics and makes the simulation more efficient. In contrast to Hartree-Fock, a nonzero value of Δ is not a signature of long-range order. Long-range order is signified by nonzero expectation values of the operators representing the order parameters.

Besides order parameters, the variational Monte Carlo method can be used to estimate a range of other physical quantities. For example, estimations of quasiparticle weights and dispersions (Paramekanti et al., 2001; Nave et al., 2006; Yang et al., 2007), Fermi surface deformations (Himeda and Ogata, 2000), stripe phases (Himeda et al., 2002), and spectral functions (Paramekanti et al., 2001; Yunoki et al., 2005) are possible. Edegger et al. (2007) provide a brief review of related work.

Besides including the essential physics, the trial wave function should also be easy to sample and easy to use for estimating the configuration energy and other observables. The sampling typically uses the Metropolis algorithm (Shiba, 1986; Yokoyama and Shiba, 1987a). A configuration state $|C\rangle$ is the state $|R\rangle = |r_{1\uparrow}, r_{1\downarrow}, r_{2\uparrow}, \ldots, r_{N\downarrow}\rangle = c^\dagger_{r_{1\uparrow}} c^\dagger_{r_{1\downarrow}} \cdots c^\dagger_{r_{N\downarrow}} |0\rangle$; that is, it is parametrized by the electron positions and spins. We accept or reject a proposed change either in position or in spin depending on whether

$$\langle \psi(R')|\psi(R')\rangle \geq \zeta \langle \psi(R)|\psi(R)\rangle,$$

where ζ is a uniform random numer in $[0, 1]$. For the Hubbard model, we almost always use

$$\sum_{k\sigma} \varepsilon_k n_{k\sigma} = -t \sum_{\langle ij\rangle\sigma} \left(c^\dagger_{i\sigma} c_{j\sigma} + c^\dagger_{j\sigma} c_{i\sigma} \right), \tag{9.21}$$

which suggests the type of configuration changes we propose. For example, we can choose the electron position randomly and then select with equal probability whether we move the electron or flip its spin. We move the electron with equal probability to a neighboring site. If our trial state is (9.12), then (Yokoyama and Shiba, 1987a)

$$\frac{\langle \psi(R')|\psi(R')\rangle}{\langle \psi(R)|\psi(R)\rangle} = g^{2\Delta N_D} \left| \frac{\det D_\uparrow(R')}{\det D_\uparrow(R)} \right|^2 \left| \frac{\det D_\downarrow(R')}{\det D_\downarrow(R)} \right|^2,$$

https://doi.org/10.1017/CBO9780511902581.010 Published online by Cambridge University Press

where ΔN_D is the change in double occupancy, and if we move the electron with spin σ at site r_j to $r_j + a$, we have

$$E(R) = \frac{\langle R|H|\psi_T\rangle}{\langle R|\psi_T\rangle} = -t\sum_{j\sigma a} g^{2\Delta N_D}\frac{\det D_\sigma\left(\ldots, r_{j\sigma}+a, \ldots\right)}{\det D_\sigma\left(\ldots, r_{j\sigma}, \ldots\right)} + UN_D.$$

We evaluate other expectation values similarly to (9.7).

The computationally expensive step is computing the ratios of the determinants. This expense would be inhibiting if it were not for a trick that reduces the cost by a factor at least equal to the order of the matrices defining the determinants. This trick is the same as the one we used in the update procedure discussed for the determinantal methods in Chapter 7. (Also see Hammond et al. (1994), appendix B.) Briefly, the inverses of the matrices D_σ are computed and stored. Then,

$$\frac{\det\left(D_\sigma + \delta D_\sigma\right)}{\det D_\sigma} = \det\left(I + D_\sigma^{-1}\delta D_\sigma\right).$$

Because we know D_σ^{-1} and the Monte Carlo move is local, δD_σ has only one row and column that are nonzero. Hence the above determinant is effortlessly calculated. Then, if the move is accepted, we use the Sherman-Morrison-Woodbury formula given in Appendix G (Press et al., 2007, chapter 2) to update D_σ^{-1}.

As stated in (9.19), $|BCS\rangle$ lies outside of the algorithm just described because it lacks a fixed number of electrons and hence is inexpressible as a Slater determinant. Formally, we amend the situation by projecting the trial state to a fixed number of electrons

$$|\psi_T\rangle = P_N P_G\,|BCS\rangle\,.$$

Examining the issue more closely we note that

$$|BCS\rangle = \prod_k\left(u_k + v_k c_{k\uparrow}^\dagger c_{-k\uparrow}^\dagger\right)|0\rangle = \exp\left(\sum_k \phi_k c_{k\uparrow}^\dagger c_{-k\downarrow}^\dagger\right)|0\rangle$$

with $\phi_k = v_k/u_k$. Expanding the exponential and keeping only the term to the P-th power, where $P = N/2$ is the number of pairs (Bouchoud et al., 1988), we obtain

$$\begin{aligned} P_N\,|BCS\rangle &= \left(\sum_k \phi_k c_{k\uparrow}^\dagger c_{-k\uparrow}^\dagger\right)^P|0\rangle \\ &= \sum_{k_1 k_2 \ldots k_P}\phi_{k_1}\phi_{k_2}\cdots\phi_{k_P}c_{k_1\uparrow}^\dagger c_{k_2\uparrow}^\dagger\cdots c_{k_P\uparrow}^\dagger c_{-k_1\uparrow}^\dagger c_{-k_2\uparrow}^\dagger\cdots c_{-k_P\uparrow}^\dagger|0\rangle \\ &= (b^\dagger)^P|0\rangle\,, \end{aligned}$$

https://doi.org/10.1017/CBO9780511902581.010 Published online by Cambridge University Press

where

$$b^\dagger = \sum_k \phi_k c^\dagger_{k\uparrow} c^\dagger_{-k\uparrow}.$$

If $\phi_k = \exp(ik\ell)$, then

$$b^\dagger_\ell = \frac{1}{\sqrt{N}} \sum_i c^\dagger_i c_{i+\ell} e^{ik\ell},$$

which has the interpretation of a sum of valence bonds in the direction ℓ.

Two electrons may pair as a singlet or a triplet. Taking $\phi(r)$ to be the Fourier transform of ϕ_k, we can show for a singlet and a triplet with $S_z = 0$ that[2]

$$\langle R| P_N |BCS\rangle = \det \phi \left(r_{i\uparrow} - r_{j\downarrow}\right),$$

where $\phi(r_{i\uparrow} - r_{j\downarrow})$ is an element of a $P \times P$ matrix (Bouchoud et al., 1988; Gros, 1988).

The state

$$|RVB\rangle = P_N P^0_G |BCS\rangle \tag{9.22}$$

with $P^0_G = \prod_i (1 - n_{i\uparrow} n_{i\downarrow})$, is the famous *resonant valence bond* state suggested by Anderson (1987). Anderson proposed that the resonant valence bond (RVB) state leads to superconductivity when preformed singlet pairs present in the parent insulating ground state of the Heisenberg model become mobile charged superconducting pairs when the system is hole doped. The study of such ground states for electronic (and quantum spin systems) in many respects has become as much a theory of matter as a suggestion for useful trial states (Edegger et al., 2007).

The trial states for electronic systems keep growing in sophistication with an accompanying increase in the number of variational parameters (Sorella, 2005; Tahara and Imada, 2008; Neuscamman et al., 2012). The overwhelming emphasis has been on unveiling the ground state of high-temperature superconductors. In high-temperature superconductors, the accompanying presence of antiferromagnetism has led to the increasing use of trial states that accommodate both types of long-range order. For example (Giamarchi and Lhuillier, 1990, 1991),

$$|\psi_T\rangle = P_N P^0_G \prod_k \left(u_k + v_k d^\dagger_{k\uparrow} d^\dagger_{-k\downarrow}\right) |0\rangle$$

with the creation operators defined by (9.17) and the coefficients defined in (9.20). In practice a variety of additional projectors can prefix $|\psi_T\rangle$. Generally, these projectors introduce additional variational parameters. Examples are given in Sorella

[2] For a triplet with $|S_z| \neq 0$, the state is a *Pfaffian* and not a determinant (Bouchoud et al., 1988).

https://doi.org/10.1017/CBO9780511902581.010 Published online by Cambridge University Press

et al. (2002); Sorella (2005); Watanabe et al. (2006); Weber et al. (2006); Tahara and Imada (2008).

While many variational Monte Carlo calculations have been performed on the single-band Hubbard model, some have addressed other models such as the periodic Anderson model (Shiba, 1986; Shiba and Fazekas, 1990; McQueen and Wang, 1991; Oguri and Asahata, 1992; Yanagisawa, 1999; Watanabe and Ogata, 2009) and three-band Hubbard models (Oguri and Asahata, 1992; Oguri et al., 1994). As evidenced in the review by Edegger et al. (2007) close behind the Hubbard model as an object of interest is the *tJ* model, which we will discuss next. It bridges the topics of Gutzwiller projected states and RVB states, the subject of the next section. It was actually for the *tJ* model that Anderson (1987) proposed (9.22) as a ground state.

tJ model

When the repulsive on-site Coulomb interaction is large, instead of projecting all double occupancy from $|\psi_0\rangle$ with P_G^0, we can alternately replace the (Hubbard) Hamiltonian with one that is equivalent to it in the limit of $U \gg t$. By "equivalent," we mean a Hamiltonian that has the same eigenvalues and the same eigenstates, up to an overall unitary transformation, as the original one. We then perform our analysis with trial states appropriate for the physics of the equivalent Hamiltonian.

From (9.11) and (9.21), we can easily convince ourselves that for $t = 0$ the number of doubly occupied sites N_D is a good quantum number, and for a given electron density the states having the smallest N_D are the states of lowest energy. These states are highly degenerate, with the degeneracy being the greatest for the half-filled case that has one electron per lattice site. Restricting our discussion to electron densities of half-filling or less, we note that $N_D = 0$ marks the states of lowest energy. In constructing an equivalent Hamiltonian, we view the kinetic energy as a perturbation breaking the degeneracy among the $N_D = 0$ states and derive the equivalent Hamiltonian by performing second-order degenerate perturbation theory.

We can perform this perturbation theory most easily by making the unitary transformation

$$H' = e^{iS} H e^{-iS} = H + \sum_{n=1}^{\infty} i^n \frac{[S_n, H]}{n!},$$

where S is some Hermitian operator and

$$S_n = [S, [S_{n-1}, H]], \quad S_1 = S.$$

Writing $H = H_0 + H_1$, we take for H_0 the Coulomb term and for H_1 the kinetic energy term. Now we expand this transformation as a power series in S,

$$H' = H_0 + H_1 + i\,[S, H_0] + i\,[S, H_1] - \tfrac{1}{2}\,[S, [S, H_0]] - \tfrac{1}{2}\,[S, [S, H_1]] + \cdots,$$

and by choosing S such that

$$H_1 + i\,[S, H_0] = 0,$$

we obtain an effective Hamiltonian

$$H' \approx H_0 + \tfrac{1}{2} i\,[S, H_1] + \cdots.$$

More generally, if we are perturbing states labeled by some quantum number n, then in a matrix representation, we would take

$$\begin{aligned} \langle n|\, S\, |n\rangle &= 0, \\ \langle n|\, S\, |m\rangle &= i \frac{\langle n|\, H_1\, |m\rangle}{E_n - E_m}, \end{aligned}$$

where $m \neq n$. For the problem at hand, the states n are those with no sites doubly occupied, and the states m are those with one or more sites doubly occupied. Those states with just one doubly occupied site dominate. In a second-quantized representation,

$$\begin{aligned} S = -i \frac{t}{U} \sum_{\langle ij\rangle,\sigma} \Big[& \left(1 - n_{i,-\sigma}\right) c^\dagger_{i\sigma} c_{j\sigma} n_{j,-\sigma} + \left(1 - n_{j,-\sigma}\right) c^\dagger_{j\sigma} c_{i\sigma} n_{i,-\sigma} \\ & - n_{j,-\sigma} c^\dagger_{j\sigma} c_{i\sigma} \left(1 - n_{i,-\sigma}\right) - n_{j,-\sigma} c^\dagger_{i\sigma} c_{j\sigma} \left(1 - n_{j,-\sigma}\right) \Big]. \end{aligned}$$

After some algebra, we arrive at

$$H_{tJ} \equiv H' = P^0_G\, (H_1 + H_2)\, P^0_G, \tag{9.23a}$$

with

$$H_2 = J \sum_{\langle ij\rangle} \left(\vec{S}_i \cdot \vec{S}_j - \tfrac{1}{4} n_i n_j \right) \tag{9.23b}$$

and

$$P^0_G = \prod_i \left(1 - n_{i\uparrow} n_{i\downarrow}\right). \tag{9.23c}$$

Here

$$S^\alpha_i = \sum_{\sigma,\sigma'=\uparrow,\downarrow} c^\dagger_\sigma \sigma^\alpha_{\sigma\sigma'} c_{\sigma'}, \quad \alpha = x, y, z,$$

where the σ^α are the Pauli spin matrices. The exchange interaction is $J = 4t^2/U^2$.

https://doi.org/10.1017/CBO9780511902581.010 Published online by Cambridge University Press

The effective Hamiltonian (9.23) is the *tJ* model. It operates only in a space where there is no double occupancy at any lattice site. As stated and used, a term dropped makes it only approximately equivalent to the Hubbard model in the large U limit. At half-filling, the lattice has an equal number of up and down electrons with one electron per site, and the *tJ* model reduces to the spin-$\frac{1}{2}$ antiferromagnetic Heisenberg model

$$H_{\text{Heisenberg}} = J \sum_{\langle ij \rangle} \left(\vec{S}_i \cdot \vec{S}_j - \tfrac{1}{4} \right), \quad J > 0. \tag{9.24}$$

Upon hole-doping away from half-filling, each site has zero or one electron (up or down) and the kinetic energy has the physical interpretation of holes hopping amid a background of antiferromagnetic fluctuations.

9.2.3 Valence bond states

With the introduction of the *tJ* model, valence bond states became prominent both as a representative of a new insulating ground state (spin liquid) and as a convenient variational basis for quantum Monte Carlo studies of Heisenberg models. Anderson suggested well prior to high-temperature superconductivity that such states are descriptors of a new type of insulating ground state (Anderson, 1973). Still prior to high-temperature superconductivity, Fazekas and Anderson suggested them as descriptors of the ground states of antiferromagnetic Heisenberg models on frustrated lattices (Fazekas and Anderson, 1974). In some sense these states have become a paradigm for novel ground states of strongly correlated electron systems that break spin-rotational and translational symmetries.

The novel ground state suggested by Anderson is the spin liquid state, a state with an energy gap and only short-range order among oppositely aligned electron spins. Some quantum spin models in one dimension have an RVB spin-liquid ground state (Majumdar and Ghosh, 1969a,b; Affleck et al., 1987, 1988), that is, a state that is a linear combination of valence bond states. Gapless spin liquids and RVB crystals are just a few of the additional proposals for novel RVB ground states. Often these states lack an order parameter. They seem especially relevant for models on frustrating lattices such as the triangular lattice. Here, we consider these states just as a convenient basis for variational Monte Carlo simulations.

In the valence bond basis, the trial state is a superposition of the valence bond states,

$$|\psi_T\rangle = \sum_V f_V |V\rangle. \tag{9.25}$$

https://doi.org/10.1017/CBO9780511902581.010 Published online by Cambridge University Press

A valence bond state is a tensor product of all possible pairs of electrons bound into singlets. These states are overcomplete, that is,

$$\sum_V |V\rangle\langle V| \neq 1, \quad \langle V|V'\rangle \neq \delta_{VV'},$$

and they number $N!/([(N/2)!]^2(N/2+1))$. Our main objective is detailing several facts about this basis that are useful in a variational Monte Carlo simulation.

A theorem of Marshall (1955) states that the ground state of the Hubbard and Heisenberg models on a bipartite lattice must have a total spin S of magnitude zero. For the Heisenberg model, the standard basis $\{|C\rangle\}$ is the set $\{|s_1, s_2, \ldots, s_n\rangle\}$ of 2^N configurations of possible eigenstates of the z-component of the spin-$\frac{1}{2}$ operator at each lattice site. It is easy to select states with total $S^z = 0$ by choosing states with half the sites having spin up and the other half having spin down, but the basis set with these states may place into the trial state expansion contributions of higher total spin. The valence bond basis is a basis with a given value of total spin. We focus only on constructing ones with $S = 0$.

We work with a tensor product state of the form

$$|(i_1,j_1)\rangle \otimes |(i_2,j_2)\rangle \otimes \cdots \left|\left(i_{N/2},j_{N/2}\right)\right\rangle = \left|(i_1,j_1)\,(i_2,j_2)\cdots\left(i_{N/2},j_{N/2}\right)\right\rangle,$$

where $|(i,j)\rangle$ is a *spin singlet* bond between lattices sites i and j. On a bipartite lattice, the convention is

$$|(i,j)\rangle = \frac{1}{\sqrt{2}}\left(\left|\left(i_\uparrow,j_\downarrow\right)\right\rangle - \left|\left(i_\downarrow,j_\uparrow\right)\right\rangle\right),$$

where i is an A-sublattice site and j is a B-sublattice site. This convention fixes the phase of the singlet. Without the phase convention we would have to keep track of the sign of the basis states as spins on the sites are exchanged. The convention also reduces the number of states in the basis to $(N/2)!$, but the basis is still overcomplete. The overcompleteness follows from the general relation

$$|(m,n)\,(k,l)\rangle + |(m,k)\,(l,n)\rangle + |(m,l)\,(n,k)\rangle = 0$$

for products of singlet states. This relation says that if the singlet pair bonds sites on the same sublattice, we can reexpress it as a sum of states where the singlets are bonding sites on different sublattices. It is straightforward to show that

$$\left(\vec{S}_i \cdot \vec{S}_j - \tfrac{1}{4}\right)|\cdots(i,j)\cdots\rangle = -\,|\cdots(i,j)\cdots\rangle\,,$$

$$\left(\vec{S}_i \cdot \vec{S}_j - \tfrac{1}{4}\right)|\cdots(i,k)\cdots(l,j)\cdots\rangle = -\tfrac{1}{2}\,|\cdots(i,j)\cdots(l,k)\cdots\rangle\,.$$

From the first equation, it follows that the magnitude of the total spin for a pair is zero, that is, $(\vec{S}_i + \vec{S}_j)^2|(i,j)\rangle = 0$.

https://doi.org/10.1017/CBO9780511902581.010 Published online by Cambridge University Press

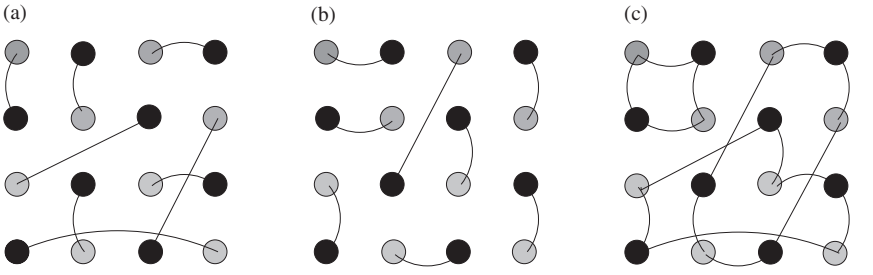

Figure 9.1 Two valence bond states (a) $|V\rangle$ and (b) $|V'\rangle$ and their overlap (c) $\langle V|V'\rangle$. The A-sublattice sites are the black dots. In the text the sites on the left edges are numbered 1, 5, 9, and 13 from the bottom up.

In Fig 9.1a and b we present two possible valence bond states for a 4×4 square lattice. The A-sublattice sites are the black dots. For convenience of discussion we will represent these states as[3]

$$|V\rangle = \begin{pmatrix} 1 & 3 & 6 & 8 & 9 & 11 & 14 & 16 \\ \underline{4} & \underline{12} & \underline{2} & \underline{7} & \underline{13} & \underline{5} & \underline{10} & \underline{15} \end{pmatrix} \tag{9.26}$$

and

$$|V'\rangle = \begin{pmatrix} 1 & 3 & 6 & 8 & 9 & 11 & 14 & 16 \\ \underline{5} & \underline{2} & \underline{15} & \underline{4} & \underline{10} & \underline{7} & \underline{13} & \underline{12} \end{pmatrix}. \tag{9.27}$$

On the top row of these arrays are the A-sublattice positions. On the bottom row are the B sites to which they are connected. This connection is the valence bond. The bond is not necessarily a physical bond. Given one member of the basis, say, $|V\rangle$, we can generate all others by permuting the $N/2$ numbers in its bottom row. With our choice of the normalization of each singlet pair,

$$\langle V|V\rangle = 1.$$

More generally,

$$\langle V|V'\rangle = 2^{N_{\text{loops}}}/2^{N/2}. \tag{9.28}$$

The latter expression says that for $\langle V|V\rangle$, $N_{\text{loops}} = N/2$. This expression also requires some explanation.

Figure 9.1c is the graph corresponding to $\langle V|V'\rangle$. It is the overlay of the graphs of Figs 9.1a and b. We see that the bonds form N_{loops} loops. In the present case $N_{\text{loops}} = 3$ and $N = 16$, so $\langle V|V'\rangle = 1/32$. If we were to define the adjoint of $|V\rangle$ by

[3] We leave it as an exercise for the readers to decipher the convention we used to number the lattice sites. (Hint: Start at the bottom left corner.)

https://doi.org/10.1017/CBO9780511902581.010 Published online by Cambridge University Press

$$\langle V| = \begin{pmatrix} \underline{2} & \underline{4} & \underline{5} & \underline{7} & \underline{10} & \underline{12} & \underline{13} & \underline{15} \\ 6 & 1 & 11 & 8 & 14 & 3 & 9 & 16 \end{pmatrix}, \tag{9.29}$$

where we now put the B sites on the top row, we could represent $\langle V|V'\rangle$ by interleaving (9.26) and (9.29)

$$\langle V|V'\rangle = \begin{pmatrix} 1 & \underline{2} & 3 & \underline{4} & 5 & \underline{6} & 7 & \underline{8} & 9 & \underline{10} & 11 & \underline{12} & 13 & \underline{14} & 15 & \underline{16} \\ \underline{5} & 6 & \underline{2} & 1 & \underline{11} & 15 & \underline{8} & 4 & \underline{10} & 14 & \underline{7} & 3 & \underline{9} & 13 & \underline{16} & 12 \end{pmatrix}.$$

In this representation the A site columns are the bonds for the ket, while the B site columns are those for the bra. Picking a site in the top row we find its bonding site in the bottom row. Taking this site back to the top row, we can find the site bonding to it. If we repeat this process until we point back to the starting site, we trace out one of the loops in the overlap graph. It is easy to demonstrate that there are only three loops in this particular case.

Besides for computing overlaps, identifying and counting loops is important because

$$\frac{\langle V|\,\vec{S}_i\cdot\vec{S}_j\,|V'\rangle}{\langle V\mid V'\rangle} = \begin{cases} 3/4, & \text{if } i,j \in \text{same loop and same sublattice,} \\ -3/4, & \text{if } i,j \in \text{same loop but different sublattices,} \\ 0, & \text{if } i,j \in \text{different loops.} \end{cases} \tag{9.30}$$

With this result we can compute the energy, the spin-spin correlation function, and the staggered magnetization, the main objects of interest for the antiferromagnetic spin-$\frac{1}{2}$ Heisenberg model.

In the valence bond basis a trial state has the form

$$\begin{aligned} |\psi_T\rangle &= \sum_V f_V\,|V\rangle \\ &= \sum_{\{i_1,j_1,i_2,\ldots,i_{N/2}\}} f_{i_1,j_1,i_2,\ldots,i_{N/2}}\,\big|(i_1,j_1)\,(i_2,j_2)\cdots\big(i_{N/2},j_{N/2}\big)\big\rangle. \end{aligned}$$

As suggested by Liang et al. (1988), we assume

$$f_{i_1,j_1,i_2,\ldots,i_{N/2}} = h(i_1,j_1)h(i_2,j_2)\cdots h(i_{N/2},j_{N/2})$$

and then invoke another theorem of Marshall (1955) that for the Heisenberg model on any bipartite lattice we can take $f_{i_1,j_1,i_2,\ldots,i_{N/2}} > 0$, and hence we can take $h(i,j) > 0$. We further assume that $h(i,j) = h(|i-j|)$. A variety of choices for h have been made. Liang et al. (1988), for example, optimized $|\psi_T\rangle$ by adjusting $h(i,j)$ over a few nearest neighbor distances and then described the remainder by adjusting the power α in a power law assumption for the function $h(i,j) \sim |i-j|^{\alpha}$. The important fact is that the trial state supports both short-range and long-range

https://doi.org/10.1017/CBO9780511902581.010 Published online by Cambridge University Press

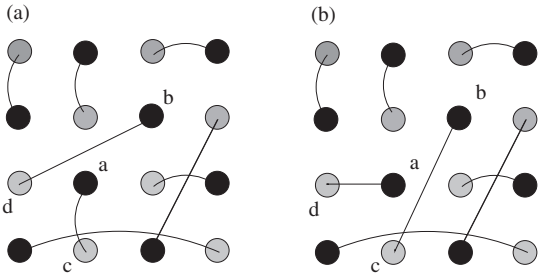

Figure 9.2 The proposed Monte Carlo move.

order depending on whether the decay is short or long range. This flexibility is one advantage of the valence bond basis.

Because the valence bond basis is nonorthogonal and overcomplete, we cannot directly use the variational Monte Carlo method described in Section 9.1.2. Instead, for those models where Marshall's positivity theorem applies, we use (9.1) and (9.25) and write

$$E_T = \frac{\sum_{VV'} f_V f_{V'} \langle V | H | V' \rangle}{\sum_{VV'} f_V f_{V'} \langle V | V' \rangle} = \sum_{VV'} H_{VV'} P_{VV'}$$

with

$$H_{VV'} = \frac{\langle V | H | V' \rangle}{\langle V | V' \rangle}, \quad P_{VV'} = \frac{f_V f_{V'} \langle V | V' \rangle}{\sum_{VV'} f_V f_{V'} \langle V | V' \rangle},$$

which suggests that we can use (9.30) to evaluate the configuration energy $H_{VV'}$ and use $f_V f_{V'} \langle V | V' \rangle$ as the sampling function. Following Liang et al., we employ the Metropolis method to do the sampling. Their suggestion was to select two A-sublattice sites, say, a and b, and then update either the $|V\rangle$ or $|V'\rangle$ associated with these sites. Let us choose $|V\rangle$. If its bond ends of the a and b sites are the sites c and d, the proposed move is creating a new state $|V''\rangle$ by interchanging the ends. We illustrate this move in Fig. 9.2. Using $P_{VV'}$, we accept the proposal according to

$$P_{\text{accept}} = \min \left\{ 1, \frac{f_{V''} \langle V'' | V' \rangle}{f_V \langle V | V' \rangle} \right\} = \min \left\{ 1, \frac{h(i_a, i_d)\, h(i_b, i_c)\, \langle V'' | V' \rangle}{h(i_a, i_c)\, h(i_b, i_d)\, \langle V | V' \rangle} \right\}.$$

We can reduce the ratio of the overlaps to

$$\frac{\langle V'' | V' \rangle}{\langle V | V' \rangle} = 2^{\Delta N_{\text{loops}}}$$

with a marked gain in efficiency. The proposed move either increases the number of loops by 1 if all sites are initially on the same loop or decreases this number by 1 if they are not. Determining which case occurs is a simple matter of a table lookup.

https://doi.org/10.1017/CBO9780511902581.010 Published online by Cambridge University Press

After accepting a move we need to update this structure. Sandvik and Evertz (2010) proposed another method with the promise of greater computational efficiency.

9.2.4 Tensor network states

We now very briefly discuss matrix product states (MPS) and projected entangled pair states (PEPS). We use the phrase *tensor network states* as an umbrella term, and a long growing list of related states is actively being developed mainly for extending the utility of the density matrix renormalization group (DMRG) method (White, 1992). A feature distinguishing these states from the ones discussed in the previous subsections is the emphasis on increasing the degree of entanglement in $|\psi_T\rangle$ within the construction of the estimate of the ground state $|\psi_0\rangle$, rather than on increasing it ex post facto by a projection operator acting on $|\psi_0\rangle$ as in, for example, a Gutzwiller state (9.12).

Until now, we have used as our basis expansion of a many-body trial wave function the form

$$|\psi_T\rangle = \sum_{i_1,i_2,\ldots,i_N} c_{i_1,i_2,\ldots,i_N} \left|\phi_{i_1}, \phi_{i_2}, \ldots, \phi_{i_N}\right\rangle, \tag{9.31}$$

where the basis state $|\phi_{i_1}, \phi_{i_2}, \ldots, \phi_{i_N}\rangle$ is a tensor product state

$$\left|\phi_{i_1}, \phi_{i_2}, \ldots, \phi_{i_N}\right\rangle = \left|\phi_{i_1}\right\rangle \otimes \left|\phi_{i_2}\right\rangle \otimes \cdots \otimes \left|\phi_{i_N}\right\rangle.$$

With this ansatz, the space of our system is a composite of N subspaces associated with the different lattice sites. Each subspace is spanned by a basis $\{|\phi_{i_j}\rangle\}$. For quantum spin systems, for example, $|\phi_{i_j}\rangle$ was one of the two eigenstates, $|\uparrow\rangle$ and $|\downarrow\rangle$, of the S_i^z spin-$\frac{1}{2}$ operator. Generally, each subspace dimension is the same. For the spin-$\frac{1}{2}$ example, this dimension is 2. In what follows we will assume it is d.

Expansions of a physical state in such composite bases are common, in part because the system dynamics is often local. For lattice models, bases built this way have the added convenience of expanding naturally as we increase the number of lattice sites. However, as the number of sites increases, the number of basis states and hence the number of terms in the expansion (9.31) increases exponentially fast. Tensor network states also use a tensor product basis in the expansion (9.31). The new ingredient is the manner in which the amplitudes of these basis states, and hence the parametrization of the trial state, is fabricated.

Let us first make a point of contrast. Approaching the fabrication of a trial state from a generalized Hartree-Fock perspective leads to the replacement of the many-body problem by an effective one-body problem whose ground state in wave-number space is very compact:

https://doi.org/10.1017/CBO9780511902581.010 Published online by Cambridge University Press

$$|\psi_0\rangle \rightarrow |k_1, k_2, \ldots, k_{\text{Nelec}}\rangle\,.$$

This state has no entanglement. Various Jastrow factors and other projectors may induce entanglement, but do so only after the construction of $|\psi_0\rangle$. The new story is putting more entanglement into the ground state a priori by approximating $c_{i_1,i_2,\ldots,i_n}$ by something other than the mean-field construct $c_{i_1,i_2,\ldots,i_n} \approx c_{i_1} c_{i_2} \cdots c_{i_N}$.

We start with the MPS in one dimension. If our system has open boundary conditions, we define an MPS by

$$|\psi_T\rangle = \sum_{\substack{i_1,i_2,\ldots,i_N \\ \alpha_1,\alpha_2,\ldots,\alpha_N}} \left[A_1^{i_1}\right]_{\alpha_1} \left[A_2^{i_2}\right]_{\alpha_1\alpha_2} \cdots \left[A_{N-1}^{i_{N-1}}\right]_{\alpha_{N-2}\alpha_{N-1}} \left[A_N^{i_N}\right]_{\alpha_N} \left|\phi_{i_1}, \phi_{i_2}, \ldots, \phi_{i_N}\right\rangle.$$

More compactly,

$$|\psi_T\rangle = \sum_{i_1,i_2,\ldots,i_N} A_1^{i_1} A_2^{i_2} \cdots A_{N-1}^{i_{N-1}} A_N^{i_N} \left|\phi_{i_1}, \phi_{i_2}, \ldots, \phi_{i_N}\right\rangle. \tag{9.32}$$

To each state at each lattice site, we associate a different matrix, except for the boundary sites where we associate row and column vectors. The matrices differ at each lattice site because with open boundary conditions the properties of the system are not uniform. If the system has periodic boundary conditions, we place the same matrix at each site and define

$$|\psi_T\rangle = \sum_{i_1,i_2,\ldots,i_N} \text{Tr}\left(A^{i_1} A^{i_2} \cdots A^{i_{N-1}} A^{i_N}\right) \left|\phi_{i_1}, \phi_{i_2}, \ldots, \phi_{i_N}\right\rangle.$$

By exploiting the extra degrees of freedom associated with the A's at each lattice site, we can entangle the states on neighboring sites and coordinate this entanglement across many sites. The order of the vectors and matrices is usually denoted by D and called the *bond dimension*. This parameter, and the imposition of physical or assumed symmetries, controls the degree of parameterization of the trial state.

For MPS, as for other tensor network states, we construct the expansion coefficients $c_{i_1,i_2,\ldots,i_N}$ not only to reflect the symmetries of the lattice model but also to maximize quantum entanglement. We expect the structure of the expansion coefficients $c_{i_1,i_2,\ldots,i_N}$ to also reflect the locality of the dynamics, for example, by being small whenever the distance between any pair of sites exceeds a few lattice spacings. If so, the small expansion coefficient reduces the importance of the associated basis state. This expectation was the justification for the pairwise factorization of the expansion coefficients for the trial state in the RVB basis. In that basis, the subsystems were the spin states on pairs of lattice sites, as opposed to spin states at individual sites, and instead of involving all possible spin states, only spin singlet states are present. The RVB states are a particular class of tensor network states. Spin singlets are entangled states.

https://doi.org/10.1017/CBO9780511902581.010 Published online by Cambridge University Press

Matrix product states naturally emerge in one dimension as the fixed-point basis of the DMRG method (Takasaki et al., 1999). This deterministic ground state method works best for models with open boundary conditions and short-range interactions defined on one-dimensional lattices or on quasi-one-dimensional systems such as few-legged ladders and Cayley trees. There is some physical insight into why the method works outstandingly well for these geometries and this boundary condition. The insight centers around the *area law* (Verstraete et al., 2008; Cirac and Verstraete, 2009).

The area law applies to systems with a gap between the ground and first excited states and short-range interactions. It says that if we consider a block A of nearest-neighbor particles (say, spins), then the information theory entropy $S = -\mathrm{Tr}\,\rho_A \ln \rho_A$ associated with the ground state's reduced density matrix for this block scales as the number of particles on the boundary of the block and not as the number inside. PEPS reduce to MPS. In both cases, we place an object at a lattice site whose number of subscripts equals its coordination number with nearest neighbor lattice sites. In two dimensions, lattice sites have a higher coordination than in one. Equally important is the fact that the number of required basis states needed scales polynomially with the size of the system. This scaling says that we in principle can construct an efficient basis from these states. Making them more efficient than they presently are is an active topic of research. In a number of cases the scaling, while polynomial, is still poor.

These basis states have also served to unveil the variational nature of the DMRG (Ostlund and Rommer, 1995; Dukelsky et al., 1998; Takasaki et al., 1999). It follows that they can be used as variational *Ansätze* in variational Monte Carlo calculations. Details of the DMRG are reviewed in Schöllwock (2005), while technical details about tensor product states and their connection to the DMRG are surveyed in McCulloch (2007), Verstraete et al. (2008), and Cirac and Verstraete (2009). Here, we will be more modest and first motivate the form of the matrix product basis and then very briefly discuss the use of tensor network states in variational Monte Carlo simulations. The use of MPS and PEPS in variational Monte Carlo simulations is a rapidly expanding topic.

To motivate the form of the MPS, we start by imagining that our system is a composite of two subsystems that have the orthonormal basis $\{|a_i\rangle\}$ spanning one subspace and the orthonormal basis $\{|b_j\rangle\}$ spanning the other. Then, creating a standard tensor product basis, we could write

$$|\psi_T\rangle = \sum_{ij} c_{ij}\,|a_i\rangle \otimes \big|b_j\big\rangle.$$

Schmidt's theorem (Nielsen and Chaung, 2000, chapter 2.5), however, says that a more compact representation exists: If a state $|\psi\rangle$ is in the composite of two

https://doi.org/10.1017/CBO9780511902581.010 Published online by Cambridge University Press

subsystems, whose spaces are not necessarily of the same dimension, then there exists an orthonormal basis $\{|u_i\rangle\}$ and $\{|v_j\rangle\}$ for the subsystems such that

$$|\psi\rangle = \sum_i \lambda_i |u_i\rangle \otimes |v_i\rangle,$$

with $\sum_i \lambda_i^2 = 1$. The λ_i are nonnegative real numbers. The number of nonzero values of λ_i is called the *Schmidt number*. It equals the dimension of the smaller of the two subspaces. If the Schmidt number equals 1, $|\psi\rangle = |u\rangle \otimes |v\rangle$ is *unentangled* (a pure state). If the Schmidt number is greater than 1, then the state is *entangled*. Accordingly, the Schmidt number is a measure of the degree of entanglement in $|\psi\rangle$. The Schmidt decomposition works for only two subsystems at a time and is unique up to a unitary transformation of any subsystem basis.

We now apply the Schmidt decomposition to the tensor product expansion (9.31), first taking one subsystem spanned by the states $\{|\phi_{i_1}\rangle\}$ and the other by the states $\{|\phi_{i_2}, \phi_{i_3}, \ldots, \phi_{i_N}\rangle\}$. Invoking Schmidt's theorem, we thus have

$$|\psi_T\rangle = \sum_{\alpha_1} \lambda_{\alpha_1}^2 |\psi_{\alpha_1}\rangle |\psi_{\alpha_1}^{[2,N]}\rangle$$

Because the basis sets $\{|\phi_{i_1}\rangle\}$ and $\{|\psi_{\alpha_1}\rangle\}$ span the same space, we can transform back to our original basis $|\phi_{i_1}\rangle$ and thus write

$$|\psi_T\rangle = \sum_{\alpha_1} \sum_{i_1} \lambda_{\alpha_1}^2 \left[\Lambda_1^{i_1}\right]_{\alpha_1} \left|\phi_{i_1}\right\rangle |\psi_{\alpha_1}^{[2,N]}\rangle.$$

Next, we apply the Schmidt decomposition to $|\psi_{\alpha_1}^{[2,N]}\rangle$ and again transform the leading state so that

$$|\psi_T\rangle = \sum_{\alpha_1,\alpha_2} \sum_{i_1,i_2} \lambda_{\alpha_1}^2 \left[\Lambda_1^{i_1}\right]_{\alpha_1} \lambda_{\alpha_2}^2 \left[\Lambda_2^{i_2}\right]_{\alpha_1\alpha_2} \left|\phi_{i_1}\right\rangle \left|\phi_{i_2}\right\rangle |\psi_{\alpha_2}^{[3,N]}\rangle.$$

Repeating these steps until we have visited every site yields a messy looking expression but one identical in form to (9.32). These steps produce a parameterization of $c_{i_1,i_2,\ldots,i_n}$ in terms of coefficients in the matrix product expansion. Clearly, the parameterization can be rich.

When we use tensor network states in variational Monte Carlo calculations, the basic algorithm remains as previously described in Section 9.1.2, with

$$P(C) = P(\phi_{i_1}, \phi_{i_2}, \ldots, \phi_{i_N}) \propto \left|\mathrm{Tr}\, A^{i_1} A^{i_2} \cdots A^{i_N}\right|^2.$$

One difference for their use is the computational cost of computing the probability ratio $P(C')/P(C)$ because of the overhead associated with the computation of the matrix products. It is important to exploit the cyclic nature of the trace operation,

https://doi.org/10.1017/CBO9780511902581.010 Published online by Cambridge University Press

store partial matrix products, and update them as opposed to the entire string of products. Details about the efficient computation of matrix elements, their products, and expectation values of operators can be found in such articles as Sandvik and Vidal (2007), Schuch et al. (2008), Sfondrini et al. (2010), and Wang et al. (2011a). The field is still evolving, and the efficiency will likely increase further.

Efficiency is often achieved by exploiting the flexibility of the tensor network concept. There is no need to restrict entanglement to nearest neighbor pairs. We can entangle the spins in a nearest neighbor plaquette of spins. In this regard we can also factorize the expansion coefficients as a product of pairs (Changlani et al., 2009; Marti et al., 2010; Boguslawski et al., 2011; Neuscamman et al., 2011; Neuscamman et al., 2012), in the manner of Liang et al. (1988) but with regularity in the placement of singlet pairs, as products of plaquettes (Sandvik, 2008; Mezzacapo et al., 2009; Mezzacapo, 2011; Wang et al., 2011b), or as products of strings (Schuch et al., 2008; Sfondrini et al., 2010). We can include triplets (Neuscamman et al., 2012) as well as singlets. We can also bring projectors back into the game. Tensor network proposals exist for variational Monte Carlo simulations of Bosons, electrons (Corboz et al., 2010a,b; Neuscamman et al., 2012), quantum spin systems, and more recently electron systems in the continuum (Marti et al., 2010; Boguslawski et al., 2011; Neuscamman et al., 2012). While our presentation was mainly from the viewpoint of one dimension, most of the computational activity focuses on two dimensions.

With the increased parameterization of the wave function, the minimization of the trial energy or its energy variance becomes a very important part of the simulations (Schuch et al., 2008; Sfondrini et al., 2010; Wang et al., 2011b). In some instances, specific optimization techniques nicely accommodate specific tensor network *Ansätze*. In other cases, the optimizations follow procedures similar to the ones we will now discuss. The focus of this discussion is a recently proposed general-purpose trial state method, suitable for problems with both small and large parameter sets and with or without Jastrow-type projectors. The work of Neuscamman et al. (2012) used this method.

9.3 Trial-state optimization

The obvious method for trial-state optimization is to minimize the variational energy evaluated on a set of Monte Carlo samples. In fact, until about 1988, this was the commonly used method. Roughly speaking, the method was to start with a good trial state $|\psi_T(p)\rangle$ that depended on a set of parameters $p = (p_1, p_2, \ldots, p_{N_{\text{opt}}})$ and then use the modulus square of this state as the distribution function in a variational Monte Carlo sampling of a set of configurations $\{C_1, C_2, \ldots, C_{N_{\text{config}}}\}$

https://doi.org/10.1017/CBO9780511902581.010 Published online by Cambridge University Press

sufficiently large so that the sum $\sum_i |\psi_T(C_i, p)\rangle / N_{\text{config}}$ approximates the ground state reasonably well. Next, with the ensemble of configurations fixed, successive sets of new parameters were generated, each having small variations relative to the previous set. A "greedy" Monte Carlo was used to accept or reject a new state depending on whether the variational energy was raised or lowered.

The downside of this method is that the number of Monte Carlo samples in the ensemble of configurations must be many orders of magnitude larger than the number of parameters being optimized. Consequently, only a few parameters could be optimized. The reason why this imbalance is necessary is that a multiple parameter trial wave function has the flexibility to fit the data well, possibly leading to parameter sets for which the variational energy on the ensemble is lower than the true energy. However, when these parameters are used to evaluate the variational energy of a new independently drawn ensemble of configurations, a much higher energy might result. Minimizing the variance of the configuration energy (Bartlett et al., 1935; Coldwell, 1977; Umrigar et al., 1988) instead of minimizing the configurational energy was found to overcome this problem. Doing this variance minimization was the standard procedure in the time period between 1988 and 2001.

More sophisticated methods that efficiently optimize the energy or, better yet, an arbitrary linear combination of the energy and the variance of the local energy now exist (Lin et al., 2000; Nightingale and Melik-Alaverdian, 2001; Schautz and Filippi, 2004; Sorella, 2005; Umrigar and Filippi, 2005; Toulouse and Umrigar, 2007, 2008; Umrigar et al., 2007). We discuss here only the most efficient of these methods, originally proposed by Nightingale and Melik-Alaverdian (2001) for optimizing both ground and excited-state trial wave functions. Their trial wave functions have linear and nonlinear dependencies on the parameters. They optimize the linear parameters by minimizing the energy and optimize the nonlinear parameters by minimizing the variance. The Nightingale approach was extended to allow optimization of both linear and nonlinear parameters by energy minimization (Toulouse and Umrigar, 2007; Umrigar et al., 2007), and then further extended to optimize an arbitrary linear combination of the energy and the variance (Toulouse and Umrigar, 2008). We focus primarily on this last optimization method and refer to it as the "linear method" even though it optimizes linear and nonlinear parameters. The various methods just mentioned were developed in the context of many-electron problems in the continuum and hence for trial states of the Slater-Jastrow form. So in the literature some algorithmic detail may focus on optimally handling this form, but the basic methods are generally applicable and in fact have been applied to lattice problems (Changlani et al., 2009).

9.3.1 Linear method

At this point, it becomes convenient to adopt the compact notation of the seminal papers. In particular, we take our configuration basis $\{|C\rangle\}$ to be the basis set $\{|R\rangle\}$ of labeled positions of N particles $R = (r_1, r_2, \ldots, r_N)$:

$$E(C) = \frac{\langle C|H|\psi_T\rangle}{\langle C|\psi_T\rangle} \rightarrow E(R) = \frac{\langle R|H|\psi_T\rangle}{\langle R|\psi_T\rangle}.$$

We next use a functional notation for projections into this basis, e.g., $\psi_T(R) = \langle R|\psi_T\rangle$. Finally we drop the subscript T so that $\psi(R) = \psi_T(R)$. We note that, as in the case with the configuration energy, when $\psi(R)$ becomes an exact eigenstate, $E(R)$ is constant and equal to the energy of that state. Thus, it is possible to optimize the trial state by minimizing the variance of the configuration energy. In the continuum, the configuration energy is called the local energy.

At each optimization step, we expand the trial wave function to linear order in $\Delta p = p - p^0$ around the current set of parameters p_0,

$$\psi_{\text{lin}}(R, p) = \psi_0(R) + \sum_{i=1}^{N_{\text{opt}}} \psi_i(R)\, \Delta p_i, \tag{9.33}$$

where $\psi_0(R) = \psi(R, p_0)$ is the current wave function (not yet the ground state) and

$$\psi_i = \partial \langle R|\psi(p)\rangle / \partial p_i|_{p=p_0} \equiv (\partial \psi(p)/\partial p_i)_{p=p_0}$$

are the N_{opt} derivatives of the wave function with respect to the parameters. This linearized wave function becomes the trial state used in the variational principle for the energy. With an infinite number of Monte Carlo samples, the optimal parameter variations Δp minimizing the energy calculated with the linearized wave function of (9.33) are the lowest eigenvalue solutions of the resulting generalized eigenvalue equation

$$H\Delta p = E\, S\Delta p, \tag{9.34}$$

where H and S are the Hamiltonian and overlap matrices in the $(N_{\text{opt}} + 1)$-dimensional basis formed by the current wave function and its derivatives $\{\psi_0, \psi_1, \psi_2, \ldots, \psi_{N_{\text{opt}}}\}$. Here, $\Delta p_0 = 1$. Drawing a finite number of Monte Carlo samples, we estimate these matrices as

https://doi.org/10.1017/CBO9780511902581.010 Published online by Cambridge University Press

$$
\begin{aligned}
H_{ij} &= \langle \psi_i | H | \psi_j \rangle = \int dR \, \frac{\langle \psi_i | R \rangle \langle R | H | \psi_j \rangle}{\langle \psi_0 | R \rangle \langle R | \psi_0 \rangle} \langle R | \psi_0 \rangle^2 , \\
&\equiv \left\langle \frac{\psi_i}{\psi_0} \frac{H\psi_j}{\psi_0} \right\rangle_{\psi_0^2} \\
&= \begin{cases} \langle E \rangle_{\psi_0^2} & \text{if } i = j = 0, \\ \left\langle \dfrac{\psi_i}{\psi_0} \dfrac{\psi_j}{\psi_0} E \right\rangle_{\psi_0^2} + \left\langle \dfrac{\psi_i}{\psi_0} E_{,j} \right\rangle_{\psi_0^2} & \text{if } i \neq 0 \text{ and } j \neq 0, \end{cases} \\
S_{ij} &= \langle \psi_i | \psi_j \rangle \equiv \left\langle \frac{\psi_i}{\psi_0} \frac{\psi_j}{\psi_0} \right\rangle_{\psi_0^2} ,
\end{aligned}
$$

where

$$
\left\langle \frac{\psi_i}{\psi_0} \frac{A\psi_j}{\psi_0} \right\rangle_{\psi_0^2} = \frac{1}{N_{\text{config}}} \sum_{k=1}^{N_{\text{config}}} \frac{\psi_i(R_k)}{\psi_0(R_k)} \frac{A\psi_j(R_k)}{\psi_0(R_k)},
$$

and

$$
E_{,j} = \frac{\partial}{\partial p_j} \left(\frac{H\psi}{\psi} \right) = \frac{H\psi_j}{\psi} - \frac{\psi_j}{\psi_0} E.
$$

On an infinite sample $\langle j \rangle = 0$ and

$$
\left\langle \frac{\psi_i}{\psi_0} E_{,i} \right\rangle_{\psi_0^2} = \left\langle \frac{\psi_j}{\psi_0} E_{,i} \right\rangle_{\psi_0^2} ,
$$

so that H_{ij} is symmetric, but this is not so on a finite sample. Since the true Hamiltonian matrix is symmetric and because a nonsymmetric generalized eigenvalue problem can have complex eigenvalues, we might think it is desirable to symmetrize the matrix. This asymmetry is actually desirable because it creates a *strong zero variance property* (Nightingale and Melik-Alaverdian, 2001) whereby the variance of each component of Δp vanishes not only in the limit of $\psi_T(R, p)$ becoming exact but also in the limit of just $\psi_{\text{lin}}(R, p)$ becoming exact, that is, in the limit of the basis states spanning an invariant subspace of the Hamiltonian. In practice, the asymmetric Hamiltonian reduces the parameter fluctuations by one to two orders of magnitude.

Updating the parameters

Part of the optimization algorithm is now in place. At each step in the iteration we linearize ψ about p_0 and estimate H_{ij} and S_{ij} by Monte Carlo sampling. Then, using readily available software, we solve the generalized eigenvalue problem for the eigenvector Δp with the lowest eigenvalue. Having obtained the parameter

https://doi.org/10.1017/CBO9780511902581.010 Published online by Cambridge University Press

variations Δp by solving (9.34), the next question is: How do we use them to update the parameters in the trial wave function?

The simplest procedure of incrementing the current parameters by Δp, $p_0 \leftarrow p_0 + \Delta p$ works for the linear parameters but will not work for the nonlinear parameters if the linear approximation of (9.33) is not good. Adjusting the parameters in ψ so it fits the optimized linear form is one possible strategy. Umrigar and coworkers suggest a simpler alternative that exploits the freedom in the normalization of the trial state. The arbitrariness in the choice of the normalization of ψ leads to an arbitrariness in the solution for the parameters. For linear parameters, the same physical wave function is obtained but with a different normalization, while for nonlinear parameters it changes the predicted wave function at each optimization step.

We now consider the differently normalized wave function $\overline{\psi}(R,p) = N(p)\psi(R,p)$ for which we require $\overline{\psi}(R,p_0) = \psi(R,p_0) \equiv \psi_0(R)$ and $N(p)$ depends only on the nonlinear parameters. Then, the derivatives of $\overline{\psi}(p)$ at $p = p_0$ are

$$\overline{\psi}_i = \psi_i + N_i\psi_0, \quad \text{where} \quad N_i = (\partial N(p)/\partial p_i)_{p=p_0}. \tag{9.35}$$

The linear approximation to $\overline{\psi}(p)$ is

$$\overline{\psi}_{\text{lin}} = \psi_0 + \sum_{i=1}^{N_{\text{opt}}} \Delta\bar{p}_i\,\overline{\psi}_i.$$

Since we obtain $\overline{\psi}_{\text{lin}}$ and ψ_{lin} by optimization in the same variational space, they are proportional to each other,

$$\overline{\psi}_{\text{lin}} = c\psi_{\text{lin}},$$

$$\psi_0 + \sum_{i=1}^{N_{\text{opt}}} \Delta\bar{p}_i\,\overline{\psi}_i = c\left(\psi_0 + \sum_{i=1}^{N_{\text{opt}}} \Delta p_i\,\psi_i\right) = c\left(\psi_0 + \sum_{i=1}^{N_{\text{opt}}} \Delta p_i\,\left(\overline{\psi}_i - N_i\psi_0\right)\right)$$

$$= c\left(\left(1 - \sum_{i=1}^{N_{\text{opt}}} \Delta p_i N_i\right)\psi_0 + \sum_{i=1}^{N_{\text{opt}}} \Delta p_i\,\overline{\psi}_i\right),$$

so $c = 1/(1 - \sum_{i=1}^{N_{\text{opt}}} \Delta p_i N_i)$ and $\Delta\bar{p}$ is related to Δp by a uniform rescaling

$$\Delta\bar{p} = \frac{\Delta p}{1 - \sum_{i=1}^{N_{\text{opt}}} N_i \Delta p_i}. \tag{9.36}$$

https://doi.org/10.1017/CBO9780511902581.010 Published online by Cambridge University Press

Also, since the rescaling factor can be anywhere between $-\infty$ and ∞, the choice of normalization can affect not only the magnitude of the parameter changes but also the sign.

We have yet to discuss the choice of the parameter gradients of the normalization factors N_i. A good choice, employed by Sorella (2005) in a different optimization method, is to choose N_i such that the parameter derivatives of the trial state $\overline{\psi}_i$ are orthogonal to ψ_0. Umrigar and coworkers employ a more general choice: They choose N_i such that

$$\left\langle \xi \frac{\psi_0}{||\psi_0||} + (1-\xi)\frac{\psi_{\text{lin}}}{||\psi_{\text{lin}}||} \middle| \bar{\psi}_i \right\rangle = 0,$$

where ξ is a constant between 0 and 1, resulting in

$$N_i = -\frac{\xi D S_{0i} + (1-\xi)(S_{0i} + \sum_j^{\text{nonlin}} S_{ij}\Delta p_j)}{\xi D + (1-\xi)(1 + \sum_j^{\text{nonlin}} S_{0j}\Delta p_j)}, \tag{9.37}$$

where $D = \sqrt{1 + 2\sum_j^{\text{nonlin}} S_{0j}\Delta p_j + \sum_{jk}^{\text{nonlin}} S_{jk}\Delta p_j \Delta p_k}$ and the sums are over only the nonlinear parameters. The choice $\xi = 0$ is that of Sorella and the choice $\xi = 1/2$ imposes the normalization of $\overline{\psi}_{\text{lin}}$ to be the same as that of ψ_0.

In the above description, we followed the formulation of Umrigar et al. (2007) in that we calculate Δp by solving the generalized eigenvalue problem with the Hamiltonian and overlap matrices in the original basis and then calculated $\Delta\bar{p}$ using (9.36). Alternatively, we could have followed the formulation in Toulouse and Umrigar (2007) and constructed $\Delta\bar{p}$ directly from the Hamiltonian and overlap matrices in the semi-orthogonalized basis. These two alternatives lead to identical parameter changes. However, if stabilization is used (a topic that will be discussed later), these alternatives lead to somewhat different parameter changes.

9.3.2 Newton's method

Before we discuss using the linear method for minimizing the energy variance, we make an important digression that unveils the linear method as a stabilized Newton method that, in practice, often converges faster than the standard Newton method.

Newton's method is a commonly used multivariate minimizer (Press et al., 2007, chapter 9). It starts by considering the truncated Taylor series expansion of the function $E(p)$ about some point p_0,

$$E(p) \approx E(p_0) + \Delta p^T \cdot g + \tfrac{1}{2}\Delta p^T \cdot h \cdot \Delta p, \tag{9.38}$$

https://doi.org/10.1017/CBO9780511902581.010 Published online by Cambridge University Press

where g is the gradient vector of E,

$$g_i = \left.\frac{\partial E}{\partial p_i}\right|_{p_0},$$

and h is the Hessian matrix of E,

$$h_{ij} = \left.\frac{\partial^2 E}{\partial p_i \partial p_j}\right|_{p_0}.$$

Minimizing this quadratic expression, we find that the optimal parameters are given by

$$\Delta p = -h^{-1} g.$$

Because $E(p)$ is not in general a quadratic function of p, it is necessary to iterate[4]

1. Solve $h \cdot \Delta p = -g$ for Δp
2. $p_0 \leftarrow p_0 + \Delta p$,

until the norm of Δp satisfies some tolerance condition (Algorithm 30).

With respect to trial-state optimization, Umrigar and Filippi (2005) provide zero-variance expressions for the gradient g and a reduced variance expression for the Hessian h, using the observation that under certain circumstances the fluctuations of a covariance $\mathrm{cov}(X, Y) = \langle (X - \langle X \rangle)(Y - \langle Y \rangle) \rangle = \langle XY \rangle - \langle X \rangle \langle Y \rangle$ of two random variables X and Y are much smaller than those of a product $\langle XY \rangle$. These zero-variance expressions typically result in a gain in efficiency of two to three orders in magnitude.

It is apparent that we can use Newton's method to minimize not only the energy but also the variance of the local energy and an arbitrary linear combination of the

Algorithm 30 Newton's method.

Input: p_0 and g_{tol} and a procedure to calculating $g_k = \frac{\partial E}{\partial p}|_{p_k}$ and $h_k = \frac{\partial^2 E}{\partial p^2}|_{p_k}$.
  $k = 0$;
  repeat
    Solve $h_k \delta p_k = -g_k$ for δp_k ;
    $p_{k+1} = p_k + \delta p_k$;
    $k \leftarrow k + 1$;
  until $\|g_{k+1}\| < g_{\mathrm{tol}}$.
  return p_{k+1}.

[4] For a multivariate quadratic form, Newton's method converges in one step. Hence it is highly efficient as it approaches the minimum. The challenge is getting near the minimum. When the eigenvalues of the Hessian range widely, the linear system of equations in Newton's method becomes difficult to solve accurately.

https://doi.org/10.1017/CBO9780511902581.010 Published online by Cambridge University Press

two. We just need to replace the expression in (9.38) with a quadratic approximation to the desired linear combination.

9.3.3 Connection between linear and Newton methods

We now establish the connection between the linear method and Newton's method (Toulouse and Umrigar, 2008). We start by reexpressing the energy (9.38) in a more revealing block matrix form

$$E(p) = \frac{\begin{pmatrix} 1 & \Delta p^{\mathrm{T}} \end{pmatrix} \begin{pmatrix} E_0 & g^{\mathrm{T}}/2 \\ g/2 & \overline{H} \end{pmatrix} \begin{pmatrix} 1 \\ \Delta p \end{pmatrix}}{\begin{pmatrix} 1 & \Delta p^{\mathrm{T}} \end{pmatrix} \begin{pmatrix} 1 & 0^{\mathrm{T}} \\ 0 & \overline{S} \end{pmatrix} \begin{pmatrix} 1 \\ \Delta p \end{pmatrix}},$$

where $\bar{S}$ is the overlap matrix and

$$\bar{H} = h/2 + E_0 \bar{S}$$

is the $N_{\mathrm{opt}} \times N_{\mathrm{opt}}$ Hamiltonian matrix in the semi-orthogonalized basis with $\xi = 0$. Minimizing this energy with respect to p yields a generalized eigenvalue equation,

$$\begin{pmatrix} E_0 & g^{\mathrm{T}}/2 \\ g/2 & \overline{H} \end{pmatrix} \begin{pmatrix} 1 \\ \Delta p \end{pmatrix} = E_{\mathrm{lin}} \begin{pmatrix} 1 & 0^{\mathrm{T}} \\ 0 & \overline{S} \end{pmatrix} \begin{pmatrix} 1 \\ \Delta p \end{pmatrix},$$

as is the case in the linear method, except that we obtain a symmetric Hamiltonian matrix.

9.3.4 Energy variance optimization

Having established the connection between the linear method and Newton's method, we now modify the linear method to optimize a linear combination of the energy and the variance of the local energy. In analogy with (9.38), all that is required is a quadratic approximation to the variance,

$$V = V_0 + g_V^{\mathrm{T}} \cdot \Delta p + \frac{1}{2} \Delta p^{\mathrm{T}} \cdot h_V \cdot \Delta p.$$

Minimization leads to the following generalized eigenvalue equation

$$\begin{pmatrix} V_0 & g_V^{\mathrm{T}}/2 \\ g_V/2 & h_V/2 + V_0 \overline{S} \end{pmatrix} \begin{pmatrix} 1 \\ \Delta p \end{pmatrix} = V_{\mathrm{min}} \begin{pmatrix} 1 & 0^{\mathrm{T}} \\ 0 & \overline{S} \end{pmatrix} \begin{pmatrix} 1 \\ \Delta p \end{pmatrix}.$$

Toulouse and Umrigar (2008) give explicit expressions for g_V and h_V.

https://doi.org/10.1017/CBO9780511902581.010 Published online by Cambridge University Press

9.3.5 Stabilization

Both in the linear method and in Newton's method, the updated parameters may be unstable if a quadratic approximation for the energy is too poor or if the number of Monte Carlo samples used to evaluate the H and S matrices is too small. We can stabilize both methods in the following manner: Newton's method is stabilized by adding a positive constant $a_{\text{diag}} \geq 0$ to the diagonal elements of the Hessian matrix, so that the proposed moves get smaller and rotate toward the steepest-descent direction. We achieve the same effect in the linear method by adding a_{diag} to the diagonal of the Hamiltonian matrix: $H_{ij} \rightarrow H_{ij} + a_{\text{diag}}\delta_{ij}(1-\delta_{i0})$. As a_{diag} becomes larger, the parameter variations Δp become smaller and rotate. We can automatically adjust the value of a_{diag} at each optimization step as follows: Once we compute the matrices H and S, we use three values of a_{diag}, differing from each other by factors of 10, to predict three new wave functions. Using correlated sampling, we then perform a short Monte Carlo run to compute energy differences of these wave functions more accurately than the energy itself. With these correlated energies we calculate a near optimal value of a_{diag}. By *correlated sampling*, we mean that instead of doing independent Monte Carlo runs to estimate related quantities, we use the N_{config} Monte Carlo configurations from a single Monte Carlo run to estimate them. The advantage is that the relative errors in these quantities is much smaller than the absolute error of the individual quantities. In our example, the related quantities are the energies of the three wave functions. We discuss correlated sampling in Appendix N.

9.3.6 Summary of the linear and Newton's optimization methods

We now summarize the linear method (Algorithm 31) and Newton's method (Algorithm 32) in a manner that emphasizes their common features. Both methods are iterative and alternate between two Monte Carlo runs. In particular, in the

Algorithm 31 Linearized optimization method.

Input: parameters p and tolerance δ.

repeat

Do a Monte Carlo run to estimate the Hamiltonian H_{ij} and overlap matrices S_{ij} ;

Solve the generalized eigenvalue problem with three values of a_{diag} to calculate three sets of rescaled parameter increments ;

Do a short Monte Carlo run with correlated sampling to calculate the relative energies of these three wave functions and thereby find a near optimal a_{diag} ;

Set $p = p_0 + \Delta\bar{p}$ using the near optimal a_{diag} ;

until $|\Delta\bar{p}| < \delta$.

return the optimized p.

https://doi.org/10.1017/CBO9780511902581.010 Published online by Cambridge University Press

Algorithm 32 Newton's optimization method.

Input: parameters p and tolerance δ.

repeat

Do a Monte Carlo run to estimate the Hessian matrix h_{ij} and the gradient vector g_i ;

Solve the linear equation with three values of a_{diag} to calculate three sets of rescaled parameter increments ;

Do a short Monte Carlo run with correlated sampling to calculate the relative energies of these three wave functions and thereby find a near optimal a_{diag} ;

Set $p = p_0 + \Delta\bar{p}$ using the near optimal a_{diag} ;

until $|\Delta\bar{p}| < \delta$.

return the optimized p.

linear and Newton methods, we first use one kind of Monte Carlo run to estimate important matrices. In the linear method, we use Monte Carlo sampling to calculate the overlap and Hamiltonian matrices. With the Hamiltonian and overlap matrices, we then solve a generalized eigenvalue equation to obtain the proposed parameter changes. To obtain the proposed parameter changes in Newton's method, we use Monte Carlo sampling to calculate the gradient vector and the Hessian matrix, and then we solve a system of linear equations. We solve either the eigenvalue problem or the linear system for three different values of a_{diag} to obtain three sets of proposed new parameters. Then, we do the second kind of Monte Carlo run that employs correlated sampling (Appendix N) to obtain the differences in the objective function (a linear combination of energy and energy variance) to greater accuracy than the individual values. Using these computed differences, we obtain a near optimal value of a_{diag} that we then use to obtain the parameters for the next iteration cycle.

Suggested reading

C. Gros, "Physics of projected wavefunctions," *Ann. Phys.* **189**, 53 (1989).

B. L. Hammond, W. A. Lester, Jr., and P. J. Reynolds, *Monte Carlo Methods for ab initio Quantum Chemistry* (Singapore: World-Scientific, 1994), chapters 2 and 5, and appendix B.

J. Toulouse and C. J. Umrigar, "Full optimization of Slater-Jastrow wave functions with application to the first-row atoms and homonuclear diatomic atoms," *J. Chem. Phys.* **128**, 174101 (2008).

J. I. Cirac and F. Verstraete, "Renormalization and tensor product states in spin chains and lattices," *J. Phys. A: Math. Theor.* **42**, 504004 (2009).

S. Sorella, "Variational Monte Carlo and Markov chains for computational physics," in *Strongly Correlated Systems*, Springer Series in Solid-State Physics **176**, ed. A. Avella and F. Mancini (Heidelberg: Springer-Verlag, 2013).

Exercises

9.1 If a trial state is accurate to $\mathcal{O}(\varepsilon)$, show that the Rayleigh quotient produces an energy estimate accurate to $\mathcal{O}(\varepsilon^2)$.

9.2 If A is a Hermitian matrix of order N and B is a Hermitian matrix defined in block form by

$$B = \begin{pmatrix} A & a \\ a^H & \alpha \end{pmatrix},$$

where a is a vector with N components and α is a scalar, show that the eigenvalues $\lambda_1 \leq \lambda_2 \leq \cdots \leq \lambda_{N+1}$ of B are interleaved by the eigenvalues of A. If A is positive definite, what is the sufficient and necessary condition that implies that B is also?

9.3 Consider a two-site electronic system without periodic boundary conditions (an H_2 molecule) and as Hamiltonian the Heisenberg antiferromagnet, the tJ model, and the positive U Hubbard model, respectively.

1. In each case analytically find the model's eigenvalues and eigenvectors, for electron fillings of one per site and less as appropriate for the model.
2. In the large U limit, map the energies and states of the Hubbard model to those of the tJ model.
3. For half-filling, connect the energies and states of the tJ model to those of the Heisenberg model.

9.4 Verify the Gutzwiller projection relation (9.13).

9.5 Instead of projecting the BCS variational wave function to a fixed N, Yokoyama and Shiba (1988) achieved the same result by a change of variables:

$$d_k^\dagger = c_{-k\downarrow}, \quad d_k = c_{-k\downarrow}^\dagger.$$

With an appropriately defined vacuum $|\bar{0}\rangle$ for the c and d particles such that $c_k|\bar{0}\rangle = d_k|\bar{0}\rangle = 0$, one finds

$$|BCS\rangle = \prod_k \left(u_k d_k^\dagger + v_k c_k^\dagger\right)|\bar{0}\rangle.$$

How is $|\bar{0}\rangle$ related to the original vacuum $|0\rangle$?

9.6 Derive (9.28), the expression for the overlap of two valence bond states, and (9.30), the expectation value of the spin-spin correlation function.

https://doi.org/10.1017/CBO9780511902581.010 Published online by Cambridge University Press